Journal of Engineering and Sustainable Development
Vol.20, No.03, May 2016
ISSN 2520-0917
www.jeasd.org

NUMERICAL AND EXPERIMENTAL INVESTIGATION OF USING INNER LONGITUDINAL FINS IN A RECTANGULAR ENCAPSULATION ON THE PCM MELTING BEHAVIORS

Dr. Jalal M. Jalil[1], Abdulmunem R. Abdulmunem[2], Akram H. Abed[3]

1) Prof., Electromechanical Engineering Department, University of Technology/ Baghdad, Iraq.
2) Assist. Lect., Electromechanical Engineering Department, University of Technology/ Baghdad, Iraq.
3) Assist. Lect., Electromechanical Engineering Department, University of Technology/ Baghdad, Iraq.

(Received: 24/11/2015 ;Accepted: 26 /01 /2016)

Abstract : In this work, the effect of using inner longitudinal fins in a rectangular encapsulation on the PCM (paraffin wax) melting process was studied numerically and experimentally. An enthalpy transformation method was used in the numerical solution to transfer the equation of energy into a nonlinear equation with a single dependent variable *H* (enthalpy) by using FORTRAN (F90) program. The discretization of energy equation with phase change problem was solved in three dimensions by using the control-volume finite-difference. A comparative study was satisfactory made between the numerical results of the enthalpy method and the experimental results with approximation ratio (10%) along the test time (90) minute. The experimental results indicated that when using inner longitudinal fins in the same rectangular encapsulations led to decrease absorber surface temperature by 10 ^{o}C. This is because part of heat energy was injected deeply in the paraffin wax by the fins. This led to accelerate melting of PCM (paraffin wax) by about 12 min in section A which is under the effect of one fin, at a distance 3 cm from the heat absorber surface. While, at section B, where two longitudinal fins have effect, melting is decelerated by about 12 min.

Keywords: *phase change materials, Enthalpy method, Finite Volume, Fin, Numerical*

تحقيق عددي وعملي لاستخدام الزعانف الطوليةً داخل التغليف المستطيل على سلوك الذوبان للمواد المتغيرة الطور

ملخص: في هذا العمل تم دراسة تاثير استخدام الزعانف الداخلية الممتدة طوليا في التغليف المستطيل على سلوك الانصهار لمادة متغيرة الطور (شمع البرافين) عددياً وعملياً. استخدمت طريقة الانثالبي في الحل العددي لتحويل معادلة الطاقة الى معادلة لا خطية مع متغير واحد وهو الانثالبي(*H*) باستخدام برنامج فورتران (F90). تم حل معادلة الطاقة ثلاثية الابعاد مع تغير الطور باستخدام الحجوم المحددة و الفروقات المتناهية. كانت المقارنة مقبولة بين النتائج العددية لطريقة للانثالبي مع النتائج العملية بنسبة تقارب (10%) على طول مدة الفحص (90) دقيقة. بينت النتائج العملية انه عند استخدام الزعانف الداخلية الممتدة طوليا لنفس التغليف المستطيل ادى الى انخفاض في درجة حرارة السطح الممتص للحرارة حوالي (10 درجة سيليزية) وّلك بسبب ان جزء من هذه الطاقة الحرارية تحقن داخليا في شمع البرافين بواسطة الزعانف, وهذا يؤدي الى التعجيل في زمن الذوبان للمادة المتغيرة الطور (شمع البرافين) حوالي (12 دقيقة) في المقطع(A) على مسافة (3 سنتيمتر) من السطح الماص للحرارة مقارنة مع التغليف المستطيل بدون زعانف. لكن عند المقطع(B) الواقع تحت تاثير زعنفتان طوليتان زمن الذوبان ارتفع حوالي (12) دقيقة مقارنة مع المقطع (A) الواقع تحت تأثير زعنفة واحدة.

*Corresponding Author abdulmunemraad@yahoo.com

1. Introduction

Latent heat storage systems play important roles for this purpose. One of the examples about that is the solar heating system used in environmental and civil engineering, where phase change materials (PCM) are utilized to store thermal energy from the sun irradiation during day and reuse the stored heat for heating air or water supply in buildings or any applications that need this heat energy. Due to latent heat of fusion in which material undergoes phase change, the Latent heat storage has higher heat storage density than sensible heat storage. For example, a rock-based sensible heat storage requires seven times the storage mass needed when using paraffin 116 wax for storing the same quantity of heat energy [1][2]. Upon reaching the PCM melting range, the Latent heat storage system undergoes isothermal operation, and the required operation temperature and duration can be controlled size through selection of the respective PCM thermo-physical properties. Due to this high heat capacity capability, this technique is utilized in cooling of electronic devices for thermal management of these electronic devices [3].

There are various methods for thermal enhancement and improvement of the heat transfer performance of latent heat storage systems [4][5]. These methods are: by using fins (extended surface), using multiple PCM's method, micro-encapsulation, and metal matrix, and metallic fillers. The use of high thermal conductive fins in thermal storage systems is one of the effective and simple methods for enhancement of the PCM melting rate in the thermal energy storage. However, increasing the metallic fins number will improve the effective thermal conductivity of the system only and will not improve the coefficient of heat transfer. This is because; the smaller fin gap size hampers the effect of natural convection heat transfer.

The performance of a rectangular PCM device with horizontal fins on vertical walls was investigated by Sezai and Gharebagi [6]. They found that, a marginal increase in heat transfer rate took place only with increasing number of fins. Thus, they concluded that, increasing number of fins will prevent the natural convection effect in the system, and melting rate becomes a conduction-dominated process. It is noted that only during phase transition (melting), natural convection becomes dominant when in liquid state and conduction heat transfer is possible in solid state.

A numerical study of the melting process of phase change materials (PCM) in a rectangular geometry by finite volume method was presented by Varol and Okcu [7]. The study was for melting in a rectangular container without fins and with 5 fins, when the wall temperature is uniform. The numerical results indicated that the transient phase change process depends on the properties of PCM, thermal condition and geometrical parameters of system. Numerical explorer of the melting and solidification of paraffin wax was done by Shatikian [8], using transient two-dimensional numerical simulations by Fluent 6.0 software to study the heat transfer rate effect on the properties of the system and on the PCM phase composition at various times.

The aim of this work is to investigate numerically and experimentally the melting behaviors and thermal performance of inner longitudinal fins in a rectangular encapsulation by finding out the temperature distributions inside paraffin wax with the

change of phase and the position of interface between liquid and solid with time comparative without fins. Based on the literature, increasing number of convectional straight fins does not improve the melting rate linearly.

2. Numerical Formulations

Heat conduction problems with phase change were represented by Stefan problems. This problem is treated by the enthalpy transforming method; this method was proposed to convert the energy equation into a non-linear equation with a single dependent variable enthalpy (H). The advantage of the enthalpy method is that the problem is formulated in a fixed region to be solved. In addition to temperature, this method treats the enthalpy as a dependent variable and discretizes the energy equation into a set of equations that contain both temperature and enthalpy.

2.1 Assumption

The analysis assumptions are:
1. Neglecting viscous dissipation,
2. Neglecting convection and radiation terms.
3. For each phase the specific heats are constant, where the phase change occurs at a single temperature. The analysis of the model in three-dimensions is related to Cao [9].The energy equation is:

$$\frac{\partial}{\partial x}\left(k\frac{\partial T}{\partial x}\right)+\frac{\partial}{\partial y}\left(k\frac{\partial T}{\partial y}\right)+\frac{\partial}{\partial z}\left(k\frac{\partial T}{\partial z}\right)+\bar{q}=\rho\frac{\partial H}{\partial t} \qquad (1)$$

and the state equation,

$$\frac{dH}{dT}=C_p \qquad (2)$$

At constant specific heat case for each phase, and the phase change occurs at a single temperature [10],

$$T=\begin{cases} T_m+H/C_{ps} & H\le 0 \quad \text{(Solid phase)} \\ T_m & 0<H<L \quad \text{(Phase change)} \\ T_m+(H-L)/C_{pl} & H\ge L \quad \text{(Liquid phase)} \end{cases} \qquad (3)$$

For the above relation, $H=0$ was selected corresponding to phase change material (PCM) in their solid state to temperature T_m.

The "Kirchhoff" temperature is introduced as [11]:

$$T^* = \int_{T_m}^{T} k(\eta)d\eta = \begin{cases} k_s(T-T_m), & T < T_m \\ 0, & T = T_m \\ k_l(T-T_m), & T > T_m \end{cases} \quad (4)$$

Transforming Equation (3), with the definition given in equation (4) results in next equation:

$$T^* = \begin{cases} k_s H / C_{ps}, & H \le 0 \\ 0, & 0 < H < L \\ k_l (H - L) / C_{pl}, & H \ge L \end{cases} \quad (5)$$

Now, introducing an enthalpy function as:

$$T^* = \lambda(H)H + S(H) \quad (6)$$

For the phase change in a single temperature,

$$\lambda(H) = \begin{cases} k_s / C_{ps}, & H \le 0 \\ 0, & 0 < H < L \\ k_l / C_{pl}, & H \ge L \end{cases} \quad (7)$$

and,

$$S(H) = \begin{cases} 0, & H \le 0 \\ 0, & 0 < H < L \\ -Lk_l / C_{pl}, & H \ge L \end{cases} \quad (8)$$

In terms of Kirchhoff temperature, Transforming equation (1) and substituting equation (6), gives:

$$\rho \frac{\partial H}{\partial t} = \frac{\partial}{\partial x}\left(\frac{\partial(\lambda H)}{\partial x}\right) + \frac{\partial}{\partial y}\left(\frac{\partial(\lambda H)}{\partial y}\right) + \frac{\partial}{\partial z}\left(\frac{\partial(\lambda H)}{\partial z}\right) + p + q \quad (9)$$

with

$$p = \frac{\partial}{\partial x}\left(\frac{\partial S}{\partial x}\right) + \frac{\partial}{\partial y}\left(\frac{\partial S}{\partial y}\right) + \frac{\partial}{\partial z}\left(\frac{\partial S}{\partial z}\right) \quad (10)$$

For the liquid region away from the moving front, Equation (9) is reduced to the normal linear energy equation:

$$\rho \frac{\partial H}{\partial t} = \frac{\partial}{\partial x}\left(k_l \frac{\partial T}{\partial x}\right) + \frac{\partial}{\partial y}\left(k_l \frac{\partial T}{\partial y}\right) + \frac{\partial}{\partial z}\left(k_l \frac{\partial T}{\partial z}\right) + q \quad (11)$$

and in the solid region, Equation (9) is reduced to:

$$\rho \frac{\partial H}{\partial t} = \frac{\partial}{\partial x}\left(k_s \frac{\partial T}{\partial x} \right) + \frac{\partial}{\partial y}\left(k_s \frac{\partial T}{\partial y} \right) + \frac{\partial}{\partial z}\left(k_s \frac{\partial T}{\partial z} \right) + q \qquad (12)$$

Without convection term in the phase change region, equation (9) is reduced to**:**

$$\rho \frac{\partial H}{\partial t} = \frac{\partial^2}{\partial x^2}(\lambda H) + \frac{\partial S^2}{\partial x^2} + \frac{\partial^2}{\partial y^2}(\lambda H) + \frac{\partial S^2}{\partial y^2} + \frac{\partial^2}{\partial z^2}(\lambda H) + \frac{\partial S^2}{\partial z^2} + q \qquad (13)$$

And for $\lambda = \lambda(H)$ *and* $S = S(H)$, the above equation employs the control-volume finite-difference. In this methodology the discretization equation is obtained by using conservation laws over finite size control volume surrounding the grid nodes. Integrating the equation over the control volumes as:

$$\iiint_{\Delta V} \rho \frac{\partial H}{\partial t} \Delta V = \iiint_{\Delta V} \frac{\partial}{\partial x}\left(\frac{\partial \lambda(H)}{\partial x} \right) \Delta V + \iiint_{\Delta V} \frac{\partial}{\partial y}\left(\frac{\partial \lambda(H)}{\partial y} \right) \Delta V + \iiint_{\Delta V} \frac{\partial}{\partial z}\left(\frac{\partial \lambda(H)}{\partial z} \right) \Delta V$$
$$+ \iiint_{\Delta V} \frac{\partial}{\partial x}\left(\frac{\partial S}{\partial x} \right) \Delta V + \iiint_{\Delta V} \frac{\partial}{\partial y}\left(\frac{\partial S}{\partial y} \right) \Delta V + \iiint_{\Delta V} \frac{\partial}{\partial z}\left(\frac{\partial S}{\partial z} \right) \Delta V + \iiint_{\Delta V} q \Delta V \qquad (14)$$

Using an explicit scheme, the time variation term becomes,

$$\iiint_{\Delta V} \rho \frac{\partial H}{\partial t} \Delta V = \rho \Delta V \left(\frac{H_p - H_p^{\circ}}{\Delta t} \right) \qquad (15)$$

For x-direction from right hand side of equation (14) becomes

$$\iiint_{\Delta V} \frac{\partial}{\partial x}\left(\frac{\partial \lambda(H)}{\partial x} \right) \Delta V = \left[\left(\frac{\partial \lambda(H)}{\partial x} \right)_e - \left(\frac{\partial \lambda(H)}{\partial x} \right)_w \right] \Delta y \, \Delta z$$
$$= \frac{\Delta y \Delta z}{(\delta x)_e} (\lambda_E H_E - \lambda_p H_p) - \frac{\Delta y \Delta z}{(\delta x)_w} (\lambda_p H_p - \lambda_W H_W) \qquad (16)$$

$$\iiint_{\Delta V} \frac{\partial}{\partial x}\left(\frac{\partial S}{\partial x} \right) \Delta V = \left[\left(\frac{\partial S}{\partial x} \right)_e - \left(\frac{\partial S}{\partial x} \right)_w \right] \Delta y \, \Delta z = \frac{\Delta y \, \Delta z}{(\delta x)_e} (S_E - S_P) - \frac{\Delta y \, \Delta z}{(\delta x)_w} (S_P - S_W) \qquad (17)$$

For *y*-direction from right hand side of equation (14) becomes

$$\iiint_{\Delta V}\frac{\partial}{\partial y}\left(\frac{\partial \lambda(H)}{\partial y}\right)\Delta V=\left[\left(\frac{\partial \lambda(H)}{\partial y}\right)_n-\left(\frac{\partial \lambda(H)}{\partial y}\right)_s\right]\Delta x\Delta z$$

$$=\frac{\Delta x\Delta z}{(\delta y)_n}\left(\lambda_N H_N-\lambda_P H_P\right)-\frac{\Delta x\Delta z}{(\delta y)_S}\left(\lambda_P H_P-\lambda_S H_S\right) \quad (18)$$

$$\iiint_{\Delta V}\frac{\partial}{\partial y}\left(\frac{\partial S}{\partial y}\right)\Delta V=\left[\left(\frac{\partial S}{\partial y}\right)_n-\left(\frac{\partial S}{\partial y}\right)_s\right]\Delta x\Delta z$$

$$=\frac{\Delta x\Delta z}{(\delta y)_n}\left(S_N-S_P\right)-\frac{\Delta x\Delta z}{(\delta y)_s}\left(S_P-S_S\right) \quad (19)$$

and for z-direction from right hand side of Equation (14) becomes

$$\iiint_{\Delta V}\frac{\partial}{\partial z}\left(\frac{\partial \lambda(H)}{\partial z}\right)\Delta V=\left[\left(\frac{\partial \lambda(H)}{\partial z}\right)_t-\left(\frac{\partial \lambda(H)}{\partial z}\right)_b\right]\Delta x\Delta y$$

$$=\frac{\Delta x\Delta y}{(\delta z)_t}\left(\lambda_T H_T-\lambda_P H_P\right)-\frac{\Delta x\Delta y}{(\delta z)_b}\left(\lambda_P H_P-\lambda_B H_B\right) \quad (20)$$

$$\iiint_{\Delta V}\frac{\partial}{\partial z}\left(\frac{\partial S}{\partial z}\right)\Delta V=\left[\left(\frac{\partial S}{\partial z}\right)_t-\left(\frac{\partial S}{\partial z}\right)_b\right]\Delta x\Delta y=\frac{\Delta x\Delta y}{(\delta z)_t}\left(S_T-S_P\right)-\frac{\Delta x\Delta y}{(\delta z)_b}\left(S_p-S_B\right) \quad (21)$$

The last term from right hand side of equation (14) becomes

$$\iiint_{\Delta V} q\Delta V=\bar{q}\,\Delta V, \quad (22)$$

Now, the coefficient of H_N, H_S, H_E, H_W, $H_T$and $H_B$as a_N , a_S , a_E , a_W , a_T *and* a_B , respectively. Writing equation (15) in the familiar standard form:

$$a_P H_P=a_N H_N+a_S H_S+a_E H_E+a_W H_W+a_T H_T+a_B H_B+b \quad (23)$$

With, H_p^o denoting the old value of H at grid point P, the values of coefficients are:

$$a_p=a_N+a_S+a_W+a_E+a_T+a_B$$

$$a_E=\frac{\Delta t}{\rho\Delta V}\frac{\lambda_E A_x}{\delta x_e},a_W=\frac{\Delta t}{\rho\Delta V}\frac{\lambda_W A_x}{\delta x_w},a_N=\frac{\Delta t}{\rho\Delta V}\frac{\lambda_N A_y}{\delta y_n},$$

$$a_S=\frac{\Delta t}{\rho\Delta V}\frac{\lambda_S A_y}{\delta y_s},a_T=\frac{\Delta t}{\rho\Delta V}\frac{\lambda_T A_z}{\delta z_t},a_B=\frac{\Delta t}{\rho\Delta V}\frac{\lambda_B A_z}{\delta z_b} \quad (24)$$

$$A_x=\Delta y\Delta z,\ A_y=\Delta x\Delta z,\ A_z=\Delta x\Delta y,\ \Delta V=\Delta x\Delta y\Delta z$$

And,

$$b=-[a_N+a_S+a_E+a_W+a_T+a_B-1]H_P^{\circ}+b_N S_N+b_S S_S+b_E S_E+b_W S_W+b_T S_T+$$
$$b_B S_B-b_P S_P+\frac{dt}{\rho}q\Delta V \quad (25)$$

in which,

$$b_P=b_E+b_W+b_S+b_N+b_T+b_B$$
$$b_E=\frac{\Delta t}{\rho\Delta V}\frac{A_x}{\delta x_e}, b_W=\frac{\Delta t}{\rho\Delta V}\frac{A_x}{\delta x_w}, b_N=\frac{\Delta t}{\rho\Delta V}\frac{A_y}{\delta y_n}, b_S=\frac{\Delta t}{\rho\Delta V}\frac{A_y}{\delta y_s} \quad (26)$$

The last procedure is similar for liquid and solid regions for equations 11 and 12. The Cartesian mesh is 31*11*11 in x, y, z directions and time step is 1 minute. Grid independence was tested by using finer mesh where the difference in temperature results is less than 1 ^{o}C.

3. Experimental Part

The system was constructed to show the effect of using the internal finned flat plate absorber of rectangular encapsulation on the PCM melting behaviors and thermal performance, compared with another flat plate absorber without fins at the same operation condition. The present work is to predict the melting behavior of PCM with and without longitudinal fins in rectangular encapsulation numerically.

3.1 System Configuration

The experimental test module shown in Figure 1a consists of 30 cm x 20 cm of aluminum flat plate absorber with thickness of 1.5 mm coated by matte black paint to absorb large amount of irradiation. The first absorber was with three internal fins (4 cm depth x 30 cm length) placed at a distance 5 cm between them. The second absorber was without fins. The 4 cm space after the absorber was filled with paraffin wax; the specifications of paraffin wax are shown in Table 1. A 30 cm x 20 cm sun simulator placed at distance 70 cm from the absorber surface.

The sun simulator was seated to give irradiation as 1200 W/m^2. Eight K-type thermocouples were used in this module as shown in Figure 1b. The first two thermocouples in sections A and B was placed inside wax at a distance 1 cm from the absorber surface. The second two thermocouples in section A and B were placed inside at a distance 3 cm from the absorber surface. The third two thermocouples were placed at the end of fins, and the fourth two thermocouples were placed at the absorber surface. Figure 2 shows the system schematic diagram.

Table 1 Physical properties of paraffin wax [12]

Specification	Value
Paraffin type	C8-H18
Melting temperature	56.8^{o}C
Specific heat of solid	2.0 kJ/kg.K
Specific heat of liquid	2.15 kJ/kg.K
Latent heat of melting	190 kJ/kg
Thermal conductivity of solid	0.24 W/m.K
Thermal conductivity of liquid	0.22 W/m.K
Density of solid at 15^{o}C	910 kg/m^{3}
Density of liquid at 70^{o}C	790 kg/m^{3}

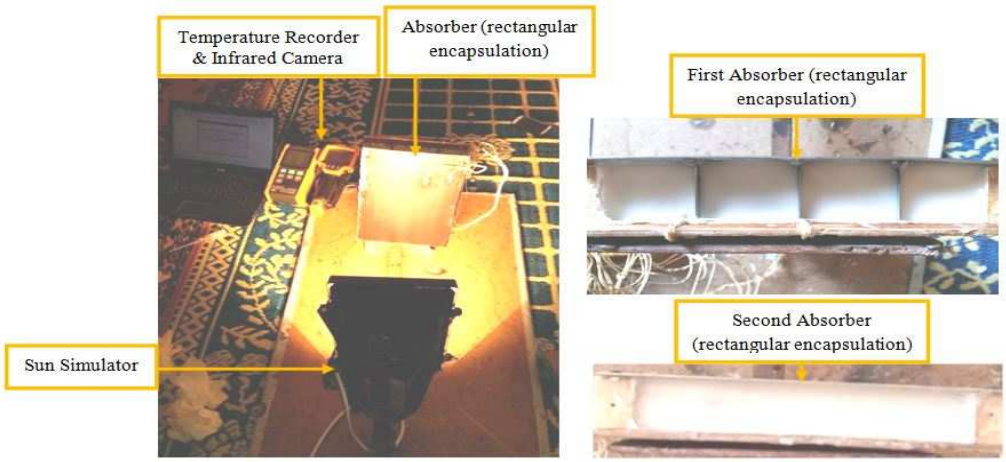

(a)

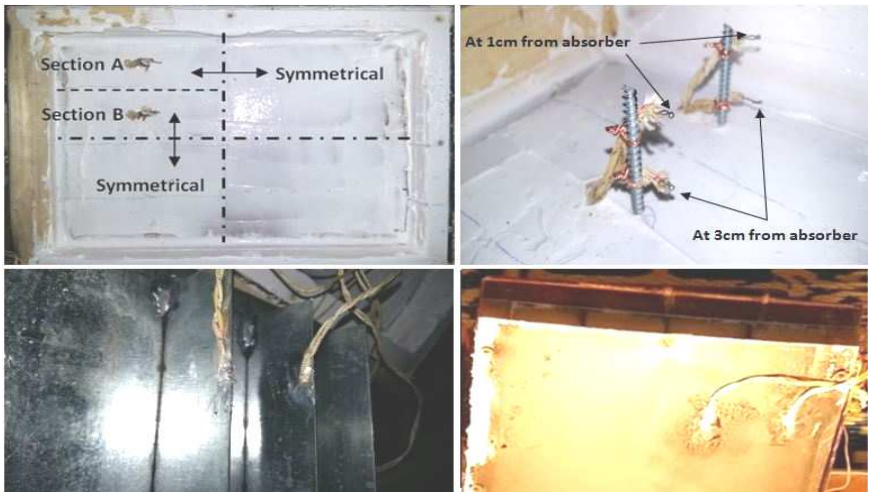

(b)

Fig. 1, (a) Experimental module, (b) Thermocouples locations

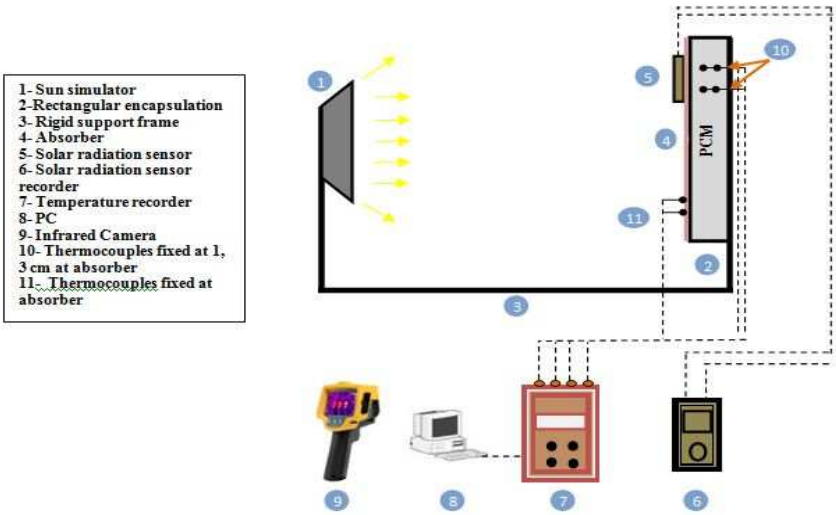

Fig. 2 Schematic diagram of the system

3.2 Experimental Measurements

The eight K-type thermocouples with accuracy (±0.4%) was connected to temperature recorder type (BTM-4208SD). The recorder accuracy is (±0.01%) andset with 5 minutes as interval time. To show the changes in behavior of paraffin wax experimentally, the infrared camera type (Fluke-Ti300) with accuracy (±2%) was used in this experiment. The irradiation value was measured by (Protek/DM 301) with accuracy (±4%)

4. Results and Discussions

The numerical results are taken from a program were built by using FORTRAN (F90) to simulate the behavior of paraffin wax with and without longitudinal fins inside the rectangular encapsulation. Figures 3 and 4 show the transient comparison between numerical results as shown in graphs (3a and 4a), and experimental results as shown in graphs (3b and 4b) were taken by the infrared camera for rectangular encapsulation with and without longitudinal fins. The numerical results show good agreement with the experimental ones approximately (10%) along the test time (90) minute.

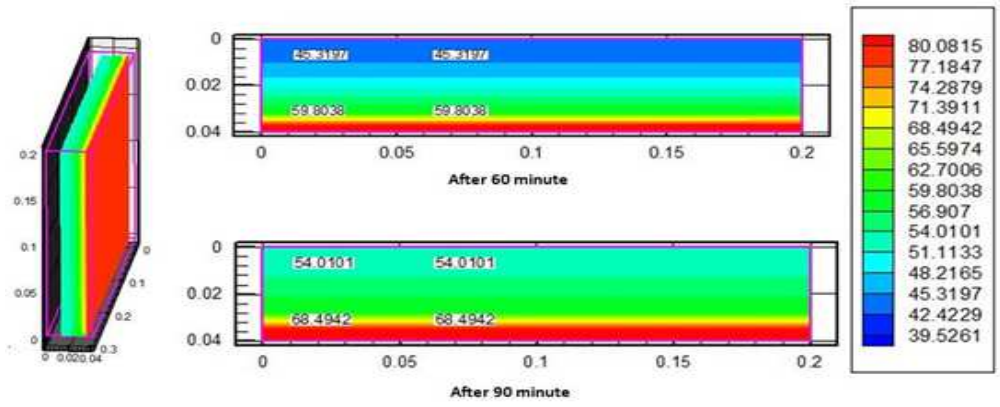

(a)

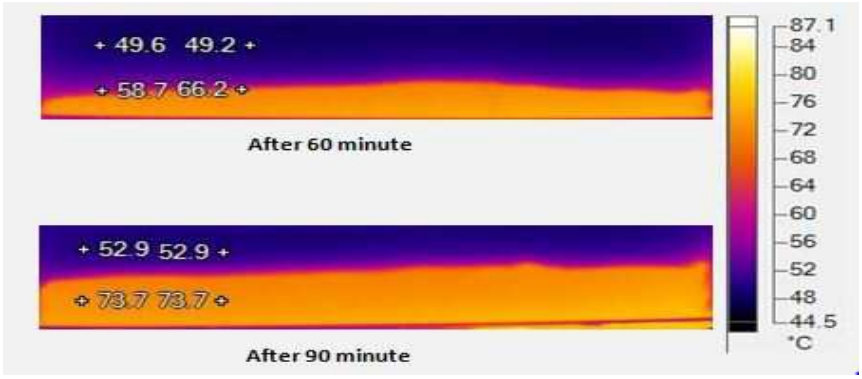

(b)

Fig. 3 Transient comparison between numerical and experimental graphs for rectangular encapsulation without longitudinal fins **(**a) Numerical graph (b) Experimental graph

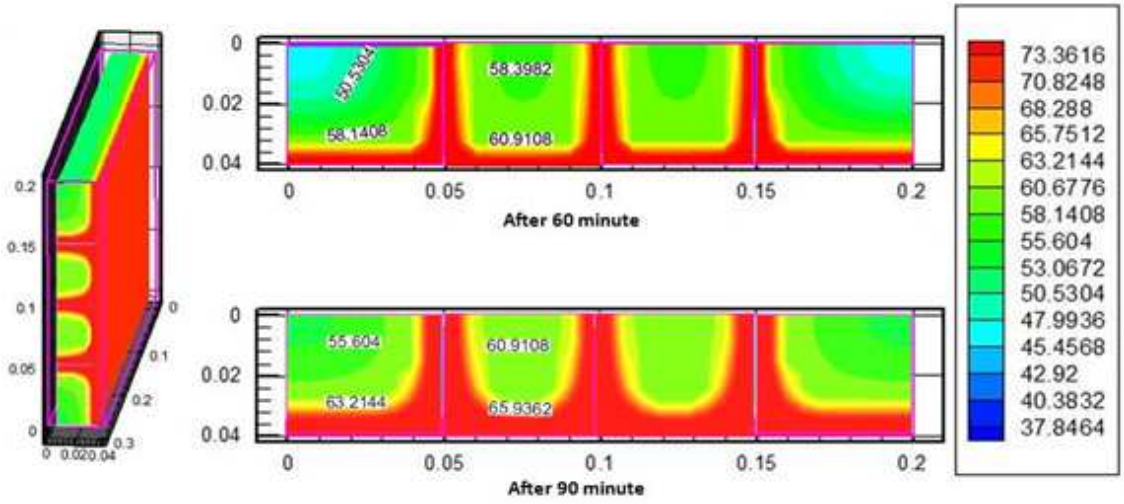

(a)

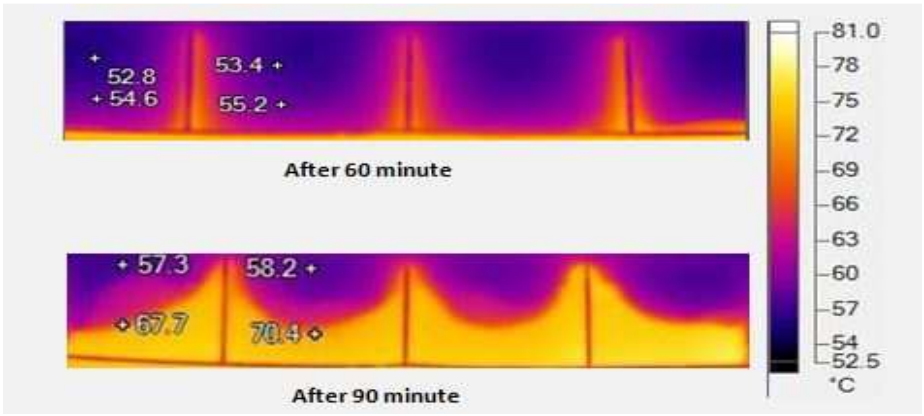

(b)

Fig. 4 Transient comparison between numerical and experimental graphs for rectangular encapsulation with longitudinal fins **(**a) Numerical graph (b) Experimental graph

The experimental data from thermocouples for both rectangular encapsulations (with and without longitudinal fins) are shown in Figures 5 and 6, respectively, to show the effect of fins on the behavior of paraffin wax, it must discuss and compare each curve of thermocouples at the same locations in Figures 5 and 6 for both rectangular encapsulations. Figure 7 indicates that the absorber surface temperature for rectangular encapsulation without longitudinal fins is higher than others by about 10 ^{o}C. This is because the heat was injected deep in the paraffin wax by the fins and this leads to drop the absorber surface temperature.

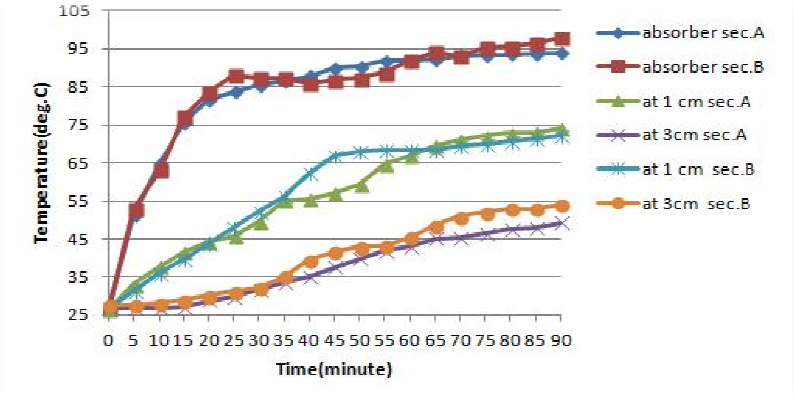

Fig. 5 Experimental thermocouples results for rectangular encapsulation without longitudinal fins

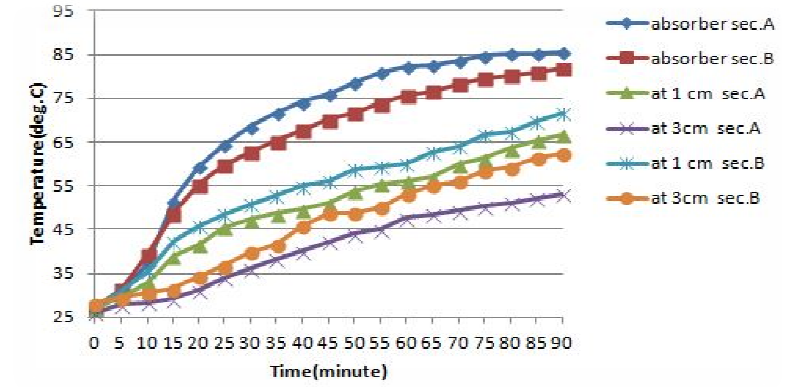

Fig. 6 Experimental thermocouples results for rectangular encapsulation with longitudinal fins

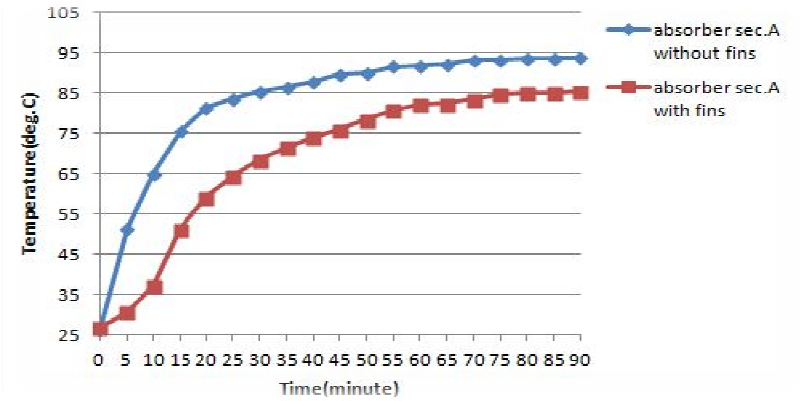

Fig 7 Experimental comparison between absorber surface temperature with and without longitudinal fins

Figure 8 shows the experimental thermocouples result inside a paraffin wax at a distance 1 cm from the absorber surface for both rectangular encapsulations (with and without longitudinal fins). The results indicate that the temperatures in the rectangular encapsulation without fins at a distance of 1 cm are higher than the others because the temperature of this absorber is highest. But in the next rectangular encapsulation with fins, the temperature at the same distance is different for different sections. It can be seen that, the temperature at section B is higher than section A. The physical explanation for this case is that the paraffin wax in section B was affected by two longitudinal fins in addition to absorber surface, but in section A, the paraffin wax was heated by one longitudinal fin in addition to absorber surface. This is clear from Figure 9 at a distance of 3cm inside paraffin wax. But it can be seen from this figure that, the temperature at this distance 3cm in rectangular encapsulation without fins is less than the others, despite it has the higher absorber temperature. This is because of the low thermal conductivity of paraffin wax which gives the advantage of using fins to inject the heat deeply inside the paraffin wax to accelerate the melting time of PCM (paraffin wax) by about 12 min in section A at the distance of 3 cm from the absorber surface compared with rectangular encapsulation without fins. But, section B is affected by two longitudinal fins, hence the melting time is increased by about 12 min compared with section A which is affected by one longitudinal fin. Figures 10, 11 and 12 show the comparison between experimental thermocouples reading and numerical predictions. They show a satisfactory agreement with error ratios fluctuated between 6 to 8 % along the time test (90) minute.

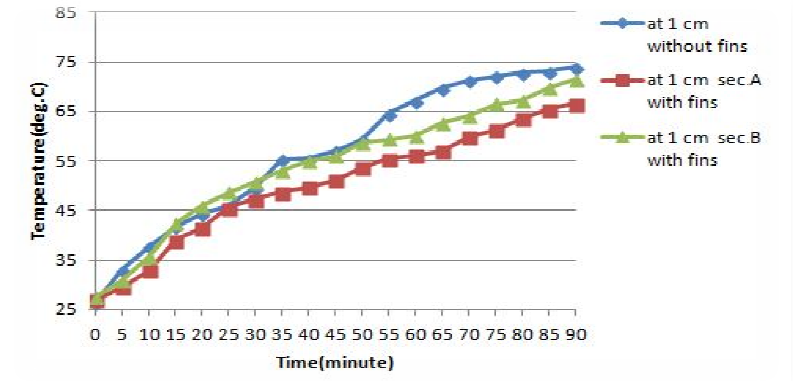

Fig 8 Experimental result for thermocouples inside paraffin wax

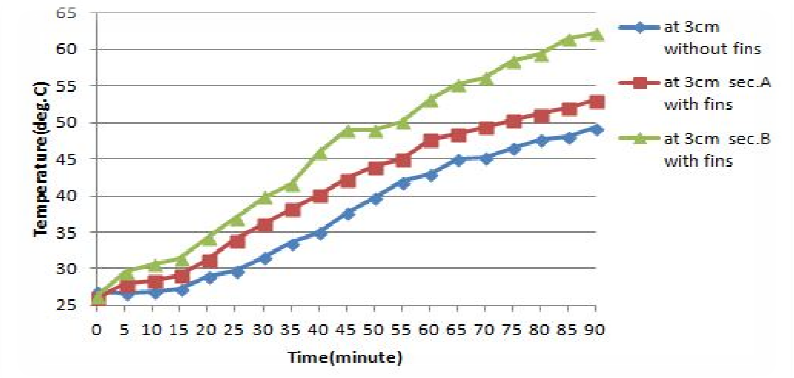

Fig. 9 Experimental result for thermocouples inside paraffin wax

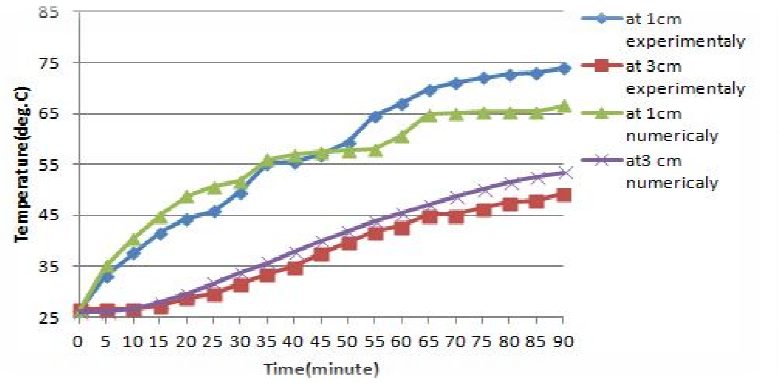

Fig. 10 Experimental and numerical comparisons for thermocouples data inside rectangular encapsulation without longitudinal fins

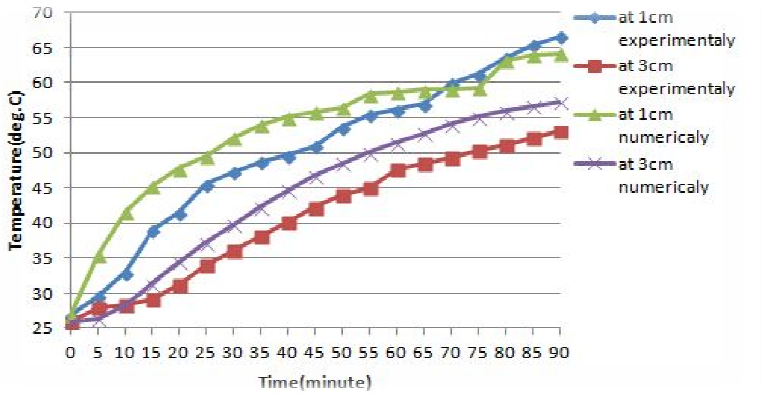

Fig. 11 Experimental and numerical comparison for thermocouples data inside rectangular encapsulation with longitudinal fins at section A

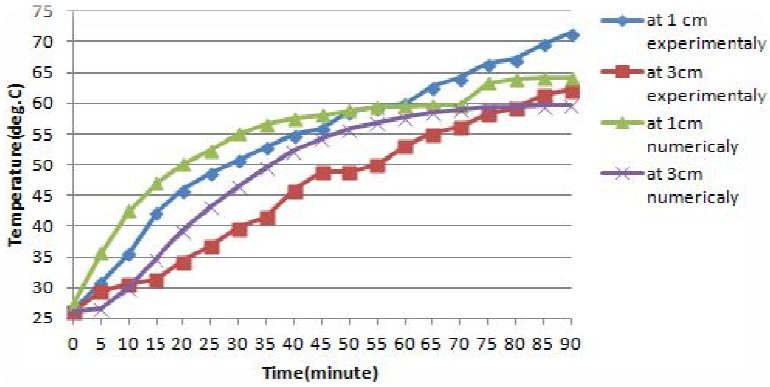

Fig. 12 Experimental and numerical comparisons for thermocouples data inside rectangular encapsulation with longitudinal fins at section B

5. Conclusions

The main important conclusions extracted from the present research can be summarized in the following:

1. The present work predicts the melting behavior of PCM with and without longitudinal fins in rectangular encapsulation numerically.
2. The using of longitudinal fins led to increase the melting time of the PCM material (paraffin wax) in the deep locations.
3. Comparison between numerical and experimental results gives satisfactory agreement, showing that the present model can predict properly the phase change processes.

Nomenclature:

A = Area (m^2)
a, b = coefficient in the discretization equation
B=‘bottom' neighbor of grid P
b=Control-volume face between P and B
C_p = specific heat (kJ/kg °C)
C_{pl} =specific heat of liquid phase (kJ/kg °C)
C_{ps} =specific heat of solid phase (kJ/kg °C)
H =Enthalpy (kJ/kg)
e= Control-volume face between P and E
E=‘east' neighbor of grid P
L=latent heat (kJ/kg)
i, j, k=Unit vector
k =thermal conductivity (W/ m °C)
k_l =liquid thermal conductivity (W/m °C)
k_s =solid thermal conductivity (W/m °C)
l=Liquid
N=‘north’ neighbor of grid P
n=Control-volume face between P and N
P=Grid point
q=Heat generation (W/m^3)
$\bar{q}$ = Average heat generation
S=‘south’ neighbor of grid P
s=Control-volume face between P and S
s=Solid
T =Temperature (°C)
t =Time(s)
T* =Kirchhoff temperature (°C)
T=‘Top’ neighbor of grid P
t=Control-volume face between P and T
T_m =melting temperature (°C)

V= Volume (m^3)
W=west' neighbor of grid P
w=Control-volume face between P and W
x, y, z =Cartesian coordinates(m)
ρ=Density (kg/m^3)
Δx, Δy, Δz = x, y, z - Direction width of the control volume
δx , δy , δz =x, y, z -direction distance between two adjacent grid points
λ = Diffusion coefficient
Δ =Difference
∂ =Partial derivative
ΔT =Temperature range (°C)

References

1. Morisson, Abdel-Kalk. (1978). "*Effect of phase change energy storage on the performance of air-based and liquid-based solar heating system*". Solar Energy, Vol.20, pp.7-67.
2. A.A. Ghonim. (1989). "*Comparison of theoretical models of phase-change and sensible heat storage for air and water-based solar heating systems*". Solar Energy, Vol. 42, pp.209-220.
3. A.G. Evans, M.Y. He, J.W. (2001). "*Temperature distribution in advanced power electronics systems and the effect of phase change materials on temperature suppression during power pulses*". J. Electron. Package.-Trans. ASME, Vol. 123, pp. 211-217.
4. S. Jegadheeswaram, S. Pohekar. (2009). "*Performance enhancement in latent heat thermal storage system: A review*". Renewable and Sustainable Energy Reviews, Vol. 13, pp. 2225-2244.
5. S. Hasnain. (1998). "*Review on sustainable thermal storage technologies, Part 1: Heat storage materials and techniques*". Energy Convers Mgmt, Vol. 39, pp.1127-1138.
6. M. Gharebagi, Sezai. (1997). "*Enhancement of heat transfer in latent heat storage modules with internal fins*". Numer Heat Transf Part A, Vol.53, pp.749-765.
7. Yasin VARO, OKCU. (2013). "*Numerical investigation of fins effect for melting process of phase change materials*". International Mechanical Engineering Congress and Exposition(IMECE), San Diego, California, USA.
8. Shatikian V., Dubovsky G., Ziskind G. (2003). "Simulation of PCM Melting and Solidification in a Partitioned Storage Unit". ASME Summer Heat Transfer Conference.
9. Cao and Faghri. (1989). "*A numerical analysis of Stefan problems for generalized multi-dimensional phase change structure using the enthalpy transformation model*". J. Heat Mass Transfer, Vol. 32, No. 7, PP. 1289-1298.
10. Norton T., Delgado A., Hogan E., Grace P. (2009). "*Simulation of high pressure freezing processes by enthalpy method*". J. Food Engineering, Vol. 91, PP: 260-268.
11. S. Cho and J. Sunderland. (1962). "*Heat-Conduction Problems with Melting or Freezing*". J. Heat Transfer, PP. 421-425.

12. Freund. M, Csikos.R, Kezthelyi.S and Mozes.Gy. (1982). "*Paraffin products : properties, technologies, applications"*. Elsvier Scientific Publishing Company Amsterdam Oxford-New York.